CANCER GENOMICS & PROTEOMICS *4*: 387-398 (2007)

IL-6 Enhances the Nuclear Translocation of DNA Cytosine-5-Methyltransferase 1 (DNMT1) *via* Phosphorylation of the Nuclear Localization Sequence by the AKT Kinase

DAVID R. HODGE[1], EDWARD CHO[2], TERRY D. COPELAND[3], TAD GUSZCZYNSKI[3], ERIC YANG[4], ARUN K. SETH[4] and WILLIAM L. FARRAR[1]

[1]*Laboratory of Cancer Prevention, Cancer Stem Cell Section, Center for Cancer Research, and*
[3]*Laboratory of Protein Dynamics and Signaling, Protein Chemistry Core Facility,*
The National Cancer Institute at Frederick, Frederick, Maryland, 21702;
[2]*Image Analysis Laboratory, Confocal Microscopy Laboratory, SAIC Frederick, Maryland 21702, USA;*
[4]*Laboratory of Molecular Pathology, University of Toronto,*
Sunnybrook Health Sciences Center, Toronto, Ontario, Canada M4N 3M5

Abstract. *The epigenetic programming of genomic DNA is accomplished, in part, by several DNA cytosine-5-methyltransferases that act by covalently modifying cytosines with the addition of a methyl group. This covalent modification is maintained by the DNA cytosine-5-methyltransferase-1 enzyme (DNMT1), which is capable of acting in concert with other similar enzymes to silence important tumor suppressor genes. IL-6 is a multifunctional mediator of inflammation, acting through several major signaling cascades, including the phosphatidylinositol-3-kinase pathway (PI-3-K), which activates protein kinase B (AKT/PKB) downstream. Here, we show that the subcellular localization of DNMT1 can be altered by the addition of IL-6, increasing the rate of nuclear translocation of the enzyme from the cytosolic compartment. The mechanism of nuclear translocation of DNMT1 is greatly enhanced by phosphorylation of the DNMT1 nuclear localization signal (NLS) by PKB/AKT kinase. Mutagenic alteration of the two AKT target amino acids within the NLS results in a major loss of DNMT1 nuclear translocation, while the creation of a "phospho-mimic" amino acid (mutation to acidic residues) restores this compartmentation ability. These observations suggest an interesting hypothesis regarding how mediators of chronic inflammation may disturb the delicate balance of cellular compartmentalization of important proteins, and reveals a potential mechanism for the induction or enhancement of tumor growth via alteration of the components involved in the epigenetic programming of a cell.*

Correspondence to: Arun K. Seth, Laboratory of Molecular Pathology, University of Toronto, Sunnybrook Health Sciences Center, Toronto, Ontario, Canada M4N 3M5, e-mail: arun.seth@utoronto.ca

Key Words: IL-6, DNMT1, nuclear translocation, AKT, inflammation, methylation.

In the human genome, approximately 4% of the cytosine residues are found in a covalently modified state resulting from the enzymatic addition of a methyl group at the fifth carbon position (1). DNA methylation is responsible for the establishment of the epigenetic "program," which functions to create tissue specific regulation and patterns of gene expression (2). The presence of 5-methylcytosine residues in DNA serves as binding sites for proteins involved in the epigenetic regulation of gene expression (3). Dysregulation of methylation patterns is a common characteristic in tumor cells, and is observed in almost all types of cancer (4). Furthermore, the loss of epigenetic integrity often results in the diminished expression of important tumor suppressor genes, apoptotic mediators, and oxidation-reduction enzymes, *via* methylation induced silencing of their promoters (5). The silencing of anticancer genes occurs through the cooperation of several factors, including the DNA cytosine-5-methyltransferases, 5-methylcytosine-DNA binding proteins (*e.g.*, MeCP1 and 2), and a group of chromatin binding and modifying proteins (6). Interestingly, the levels of DNMT1 expression are elevated in tumor cells (7).

Extracellular stimulation of cells resulting in dysregulation of DNMT1 expression patterns could conceivably exacerbate the epigenetic silencing of anticancer genes by acting to produce higher than normal levels of the enzyme's expression. The inflammatory cytokine Interleukin-6 (IL-6) is a known activator of the phosphatidylinositol-3-kinase (PI-3 kinase) signaling pathways, and subsequently is capable of activating AKT, an anti-apoptotic kinase (8, 9). Previously,

it was shown that IL-6 induced the expression and activity of DNMT1 in K-562 cells (10, 11); and played a role in the maintenance of promoter methylation in multiple myeloma cell lines (12), as well as cholangiocarcinoma cells (13). AKT kinase activity has been implicated in the pathophysiology of many tumors, including multiple myeloma, prostate, liver, and others (14, 15). AKT targets the $p21^{WAF1/CIP1}$ tumor suppressor protein, which in the unphosphorylated state inhibits DNA replication (16). AKT-dependent phosphorylation of $p21^{WAF1/CIP1}$ at Thr 145 prevents the complex formation of $p21^{WAF1/CIP1}$ with PCNA, thus making PCNA available for "other" potential binding partners, such as DNMT1 (17). Phosphorylation by AKT is capable of preventing the cytoplasmic to nuclear translocation of other important cell cycle and apoptotic proteins, either by directly phosphorylating the protein as in the case of $p27^{KIP}$, the kinase inhibitor protein (18) or by phosphorylating an associated protein such as MDM2 in the case of p53, a key mediator of apoptosis (19).

In order to methylate DNA, the DNMT1 enzyme must be translocated into the nucleus where it binds to proliferating cell nuclear antigen (PCNA) *via* an N-terminal recognition domain, forming a stable heteromeric complex (20). Typically, the alpha and beta importins comprise an integral part of the nuclear transport mechanism by binding to the nuclear localization signal (NLS) present on the target protein. Such a NLS region has been identified in the mid-N-terminal region of the DNMT1 protein, and verified by deletion analysis (21). Interestingly, there are reports showing that phosphorylation of serine, and threonine residues found within or adjacent to the NLS can affect this translocation mechanism, probably by altering the affinity of the target protein for accessory proteins (*e.g.*, importins) required for normal transport function (22, 23). Furthermore, disturbing the normal mechanisms of nuclear translocation may contribute to the development or enhancement of tumor growth (24, 25).

Very little is known regarding the phosphorylation status of numerous potential kinase target sites within the DNMT1 protein, or whether the protein undergoes transient phosphorylation events that affect its function. DNMT1 was demonstrated to undergo phosphorylation *in vitro* by protein kinase C, but this result was generated *in vitro* with purified proteins (26). A later report demonstrated a single phosphorylation site in murine DNMT1 at Serine 514, after labeling murine erythro leukemia (MEL) cells for 12 hours with 10 mCi of ^{32}P-orthophosphate (27). Definitive identification of other sites of phosphorylation by mass spectroscopy was not possible due to the small amounts of phosphopeptides present in the immunoprecipitated protein, but phosphothreonine was also observed in thin-layer chromatography analysis, indicating the presence of other phosphorylated sites (27).

In this report, we present data that the cytoplasmic to nuclear translocation of DNMT1 is increased by the treatment of cells with IL-6. Computer analysis of the peptide sequence of the DNMT1 enzyme revealed two high-probability, putative AKT target sites close to the NLS. We also demonstrate that stimulation of the PI-3 kinase pathway, and subsequent activation of AKT by IL-6, can in fact mediate the phosphorylation of these two AKT target sites within or adjacent to the DNMT1 NLS region. Moreover, we show that removal of these two AKT target amino acids abrogates the translocation of a DNMT1:EGFP fusion protein, probably by affecting the affinity of importin binding to the protein. Conversely, the creation of a phospho-mimicing amino acid (changing to an acidic, negatively charged residue) allows efficient translocation without the addition of IL-6 (28).

Materials and Methods

Construction and site-specific mutagenesis of the DNMT1:EGFP and DsRED2 fusion proteins. The first 396 codons of the human DNA cytosine-5-methyltransferase-1 (DNMT1) protein (Genbank NM_001379) were subcloned into the BamH1 restriction endonuclease site in the polylinker of pEGFP-N1 #6085-1 (BD Biosciences, 2350 Qume Drive, San Jose, CA 95131, USA); Genbank Accession U55762) creating an in-frame fusion protein with DNMT1 codons at the amino terminus of the protein, and the EGFP protein at the carboxyl terminus. PCR primers (5'-GGGATCCAGAGATGCCGGCGC-GTACC-3' sense) and (5'-TGGATCCGCGGGAAGCGCCTCATA-3' antisense) were synthesized to create BamH1 sites at the ends of the amplified fragment to facilitate cloning. An analogous construct was created using the same DNMT1 fragment and restriction sites with the DsRed2-N1 expression vector (BD Biosciences #6973-1). Both vectors contained neomycin-resistance cassettes (*neo*^{r}) selectable by G-418. A truncated version of the DNMT1:EGFP fusion protein, beginning immediately after the PCNA site (AKRKPQ, 4th line of the amino acid sequence Figure 1A) was also created to remove the putative the PCNA binding motif. The amino-terminal PCR primer used to generate this construct (5'-GGGATCCATG GCCAAACGGAAACCTCAGG-3') was used in combination with the same carboxyl terminal PCR primer used for the 396 amino-acid construct. Site-specific mutagenesis was performed in the regions of the two putative AKT sites using matched sets of PCR primers (sense and antisense), both containing a single nucleotide difference at the point of the desired mutation. Primers used to mutate the target serine of first putative AKT site (RRRVT**S**R to RRRVT**A**R) were (5'-GAGACGTAGAGTTACAGCCAGAGA ACGAGTTGC-3' sense) and (5'-GCAACTCGTTCTCTGGCT GTAACTCTACGTCTC-3' antisense); for (RRRVT**S**R to RRRVT**D**R) the primers were (5'-GAGACGTAGAGTTACAG ACAGAGAACGAGTTGC-3' sense) and (5'-GCAACTCGTT CTCTGTCTGTAACTCTACGTCTC-3' antisense). Primers used to mutate the target threonine of the second putative AKT site (RLRSQ**T**K to RLRSQ**A**K) were (5'-GAGACTCCGAAGTCAA GCCAAAGAACCAACACC-3' sense) and (5'- GGTGTTGG TTCTTTGGCTTGACTTCGGAGTCTC-3' antisense); for (RLRS Q**T**K to RLRSQ**D**K) the primers were (5'-GAGACTCCGAAGT

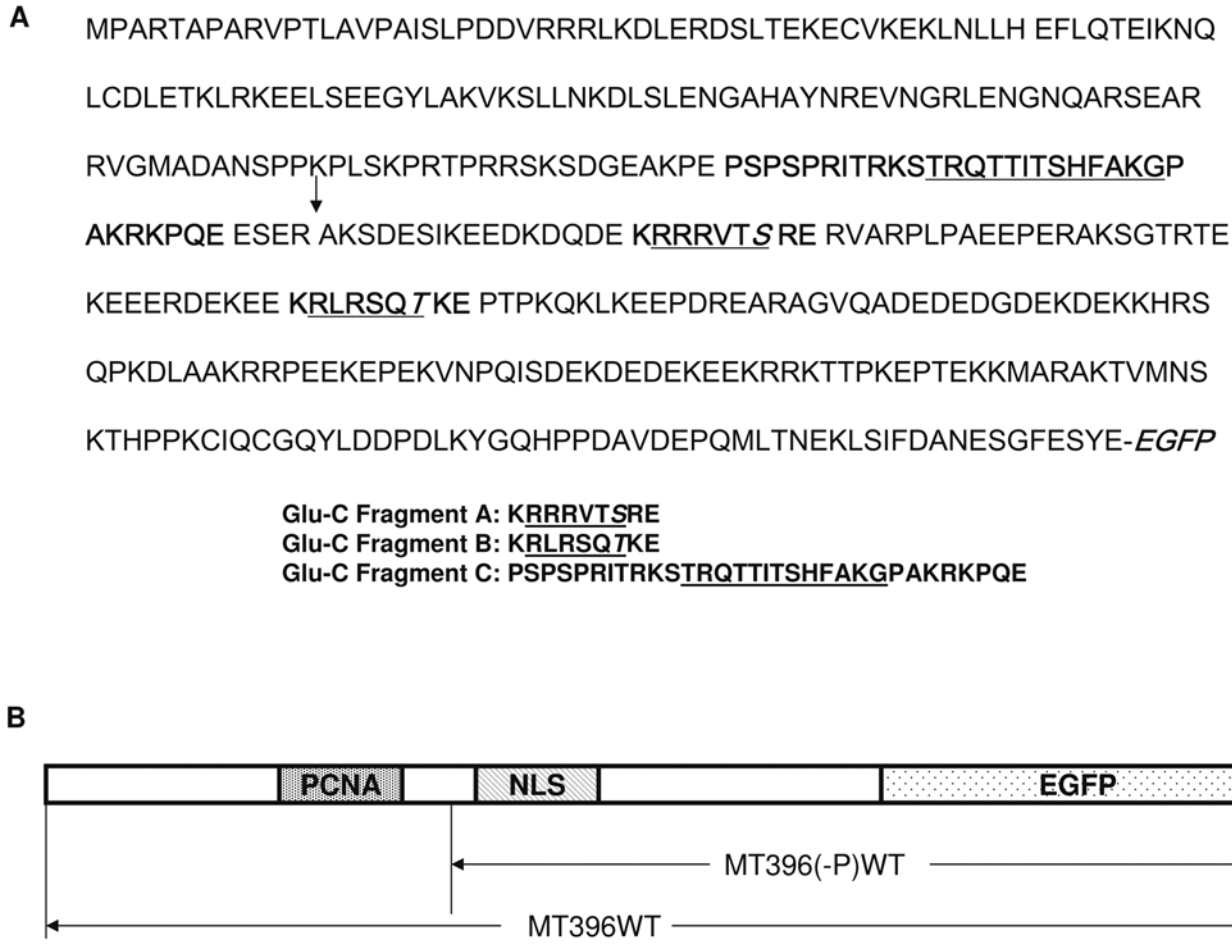

Figure 1. *Sequence analysis of the DNMT-1 regulatory domain and creation of DNMT1:EGFP fusion constructs. Panel A. Amino acid sequence of the first ~396 residues of the human DNA cytosine-5-methyltransferase 1 protein (DNMT1), fused in-frame at the carboxyl terminus with the extended green fluorescent protein. Two putative target sites for the AKT kinase (RxRxxT/S) in close proximity to the nuclear localization signal (NLS) are underlined, as is the binding site used by proliferating cell nuclear antigen (PCNA). Three peptides containing putative phosphorylation sites generated by cleavage with the Glu-C protease are also shown in bold and below. Relative positions of the PCNA binding site, the NLS, and the carboxy-terminal EGFP tag on the full-length construct are shown in Panel B; the start position of the PCNA truncated (minus-P) construct is indicated by an arrow in the text.*

CAAGACAAAGAACCAACACC-3' sense) and (5'-GGTGT TGGTTCTTTGTCTTGACTTCGGAGTCTC-3' antisense). Each mutated construct was checked by automated dye sequencing for the entire length of the protein to confirm the presence of the desired amino acid change and the integrity of the remaining protein sequence.

Co-immunoprecipitations using DNMT1:EGFP as bait. Using monoclonal antibody (MAb) specific for green fluorescent protein (*Aequorea victoria*), (Roche Applied Science, Indianapolis, IN 46250, USA; Cat.# 11 814 460 001), cells expressing the DNMT1:EGFP fusion protein were harvested in ice-cold PBS containing phosphatase, and protease inhibitor cocktails (Sigma-Aldrich, Inc., PO Box 14508, St. Louis, MO 63103, USA; Cat.#s P5726 and P2850; Cat.# P8340); then lysed and clarified by centrifugation in 1% TX-100 Tris-HCl pH 7.4, with 150 mM NaCl, 1 mM $MgCl_2$ and fresh inhibitors added. After pre-clearing with protein-G-sepharose for one hour, anti-EGFP MAb covalently linked to protein-G-sepharose was added to immunoprecipitate the DNMT1:EGFP fusion proteins along with any binding partners. The precipitated proteins were separated on an 8-16% SDS-PAGE gel and probed using antibodies specific for either alpha-importin Cat.# R43020-050 or beta-importin Cat.# K48020-050 (BD Biosciences-Transduction Laboratories). In other experiments, immunoprecipitated proteins were subjected to Isoelectric Focusing/SDS-Page 2D-Gel electrophoresis (PROTEAN, Bio-Rad Laboratories, Hercules, CA 94547, USA). To visualize proteins, either colloidal coomassie blue, silver staining, or in certain instances, Diamond Stain (for phosphorylated proteins) (Invitrogen-Molecular Probes, Eugene, OR 97402, USA; Cat.# 33300) were used.

Fluorescent recovery after photobleaching (FRAP). Stable cell lines expressing the DNMT1:DsRED2 fusion protein were created and rates of translocation from the cytoplasm to the nucleus using

fluorescence recovery after photobleaching analysis (FRAP) were determined (29). Due to previously encountered issues of phototoxicity with the EGFP fusion constructs, we opted to use the DNMT1:DsRED2 expression vector, created by cloning the identical region of DNMT1 as described above, into the DsRED2 expression vector, thus creating the same fusion vector used in other experiments. By photobleaching the entire nucleus and performing a single exponential analysis, the differences between nuclear-cytoplasmic transfer rates for cells stably transfected with DNMT1:DsRED2 were determined throughout a range of conditions (30). Cells of uniform fluorescent intensity were chosen for analysis to ensure that neither over-expressing nor under-expressing cells were used. Cells were serum deprived overnight prior to imaging; then stimulated with 100 ng/mL IL-6 1 hour before FRAP analysis; negative controls consisted of IL-6 deprivation. Cells were imaged with a 40x oil immersion objective lens. Photobleaching was performed using 514 nm and 543 nm laser lines to reduce the number of iterations for bleaching and overall bleach time. Images were collected using the 543 nm laser line and a LP560 emission filter was used for image acquisition. Three pre-bleach images were acquired to determine the rate of unintentional photobleaching due to laser exposure during normal image acquisition. After photobleaching, recovery images were acquired with no pause between the image acquisitions for the first five minutes, after which the temporal resolution was changed to acquire images every five minutes for a total image acquisition time of thirty minutes. In some experiments, Triciribine (AKT Inhibitor V, API-2) (EMDBiosciences, La Jolla, CA 92039, USA; Cat.# 124012) a specific inhibitor of AKT Kinase activity was used at a concentration of 1 μM to study the nuclear translocation of DNMT1 following IL-6 stimulation (31).

Image analysis and quantification. MIPAV image analysis software (CIT/NIH, Bethesda, MD 20817, USA) was used for the interpretation of FRAP analysis data. Single exponential analysis was performed comparing the whole cell *versus* the nuclear intensities. At least ten cells per treatment condition were acquired and analyzed to ensure statistical significance. The half-lives ($t_{1/2}$) were averaged together for each sample to determine a change in rate due to treatment. In a single exponential two-compartment analysis, the half-life was inversely proportional to the number of proteins-per-second (S) that entered the nucleus. Therefore, a lower half-life translates to a higher number of proteins entering the nucleus per second. Images were corrected for inherent photobleaching over time by choosing a cell in the same field of view that was not deliberately photo-bleached, and images were also background corrected using an area of the image that did not contain any cells. Data points were normalized by bringing the first point in the series to zero for all data sets to allow a more direct comparison between the different samples. Region of interests (ROIs) for the bleached regions (*i.e.* nuclei) were automatically drawn by the MIPAV software and corrected where necessary. Whole cell ROIs were drawn manually, determined by differential interference contrast (DIC) images of cell morphology.

Identification of phosphoserine-209 of DNMT1 by mass spectrometry. Monoclonal antibody specific for EGFP (Roche Applied Science, Indianapolis, IN 46250, USA) was covalently cross-linked to protein-G-sepharose beads and the resulting affinity resin was used to immunoprecipitate DNMT1:EGFP fusion protein. The affinity resin and adherent proteins were separated by SDS-PAGE, and the gel was stained with G-250 coomassie blue. The DNMT1:EGFP fusion protein band was verified to be DNMT1 by parallel gel western blotting, and peptide microsequencing through tandem mass spectrometry. The DNMT1 protein band was excised and in-gel digested according to the previously published procedure (32). Sufficient amounts of Trypsin (Promega, Madison, WI 53711, USA), V8 (Sigma-Aldrich), or Lys-C (Roche) dissolved in 50 mM ammonium bicarbonate (NH_4HCO_3) at 12.5 ng/μL were used to rehydrate the gel pieces and digest the DNMT1. The digested protein was desalted by C18 Zip-tip (Millipore Corp. Billerica, MA 01821, USA) and eluted with 1.5 μL of 50% acetonitrile containing α-cyano-4-hydroxycinnamic acid (4 mg/mL) for MALDI tandem mass spectrometry analysis (QSTAR-XL, Applied Biosystems/MDS Sciex, Foster City, CA 94404, USA).

Phosphoamino acid analysis. Stable HEK-293 cell lines expressing either the wild-type or DD mutant DNMT1:EGFP fusion proteins were rested overnight in 1% FBS, then loaded with 1 mCi of ^{32}P orthophosphoric acid in phosphate free medium for 15' at 37˚C, followed by stimulation with IL-6 for 30' at 37˚C. Cells were scraped into ice-cold PBS containing phosphatase and protease inhibitor cocktails, centrifuged and lysed in 1% TX-100 Tris-HCl pH 7.4, with 150 mM NaCl, 1 mM $MgCl_2$ with inhibitors. After pre-clearing with protein-G-sepharose for one hour, anti-EGFP MAb covalently linked to protein-G-sepharose was added to immune-precipitate the DNMT1:EGFP fusion proteins. The IPs were then separated on PAGE-SDS gels and electroblotted onto PVDF filter, which was exposed to X-ray film, or stained with colloidal coomassie blue stain to visualize the bands of interest. Some of the labeled protein was subjected to in-gel digestion as above with Glu-C protease (Roche) dissolved in 50 mM ammonium bicarbonate (NH_4HCO_3) at 12.5 ng/μL, with the digested peptides retained for HPLC phosphopeptide mapping analysis. Other portions of the membrane containing the labeled DNMT1:EGFP fusion proteins were hydrolyzed in 200 ml 4 N HCl at 110˚C for 1.5 h. Phosphoamino acid standards were added and the solution was lyophilized. The contents were re-dissolved in electrophoresis buffer (acetic acid / formic acid / water, 15 / 5 / 80, v / v / v) and applied to 20x20 cm cellulose TLC plates. The plate was electrophoresed at 1500 v for 40 min then rotated 90˚ and subjected to chromatography overnight using 0.5 M NH_4OH / isobutyric acid, 30 / 50, v / v. The plate was dried and sprayed with ninhydrin to localize the phosphoamino acid standards. Radioactivity was detected and visualized with a Typhoon Model 9200 phosphoimager (Amersham Biosciences, Piscataway, NJ 08855) (33).

Phosphopeptide mapping. Membrane containing labeled DNMT1:EGFP fusion protein was cut into small pieces and washed sequentially with methanol, distilled water and then blocked with 1.5% PVP-40 in 100 mM acetic acid. Membranes were digested with either trypsin or Glu-C (Roche) proteases in 50 mM NH_4HCO_3 pH 8 overnight. Supernatants containing released peptides were removed, adjusted to pH 2 with 20% aqueous trifluoroacetic acid and subjected to reversed phase high performance liquid chromatography (HPLC) on a Waters 3.9x300 mm C_{18} column. The column was developed with a gradient of 0-30% acetonitrile in 0.05% aqueous trifluoroacetic acid over 90 min at a flow rate of 1 mL/min. One ml fractions were collected and counted for ^{32}P in a

Beckman 6500 scintillation counter (Beckman Coulter, Inc., Fullerton, CA 92834) (34). ^{32}P labeled peptides were coupled to Sequalon disks and subjected to solid phase Edman degradation with a Model 492 Applied Biosystems peptide sequencer (Applied Biosystems, Foster City, CA 94404, USA). Cycle fractions were collected onto Whatman #1 paper discs and radioactivity was quantitated using a Typhoon phosphoimager (Amersham Biosciences, Piscataway, NJ 08855, USA).

Confocal microscopy imaging of native DNMT1 and DNMT1: EGFP nuclear translocation. Cells were grown overnight on tissue culture slides and transfected with the appropriate DNMT1:EGFP fusion protein expressing plasmid. The next morning, cells were rinsed with PBS pH 7.4, then fixed for ten minutes at room temperature in 0.22 μM filtered PBS pH 7.4, containing freshly prepared 4% paraformaldehyde. Cells were then rinsed twice with PBS pH 7.4 (five minutes per rinse) and made permeable by treating them with 0.2% Triton X-100 in PBS pH 7.4 for 10 minutes, at room temperature. For native DNMT1 immunohistochemistry labeling experiment, anti-DNMT1 Mab IMG-261A (Imgenex, San Diego, CA 92121, USA) was used to probe HEK293 cells that were serum deprived overnight, then stimulated with 100 ng/mL IL-6 4 hours before imaging; negative controls received no IL-6. In both the labeling and visualization of expressed proteins, DAPI was added to counterstain the nuclei; next, cover slips were added to the slides and the edges sealed with clear plastic sealer. Confocal Microscopy (Zeiss LSM 510) (Carl Zeiss IMT Corporation Maple Grove, MN 55369, USA) was used to generate the images; separate plates for DAPI and EGFP demonstrate translocation.

Results

Sequence analysis of the DNMT-1 regulatory domain and creation of DNMT1:EGFP fusion constructs. We analyzed the peptide sequence of the first ~396 amino acid residues of the human DNMT1 enzyme for any uncharacterized phosphorylation sites (Figure 1A), and observed numerous potential targets for post-translational modification by protein kinases. The amino-terminal region of the DNMT1 enzyme contains two important structural motifs; the proliferating cell nuclear antigen (PCNA) binding site (TRQTTITSHFAKG), and the Nuclear Localization Sequence (NLS) (DQDEKRRRVTSRERVARPL) (Figure 1A and B). We observed two potential AKT target sites, one within the actual NLS region (AKT site shown in bold font) (DQDEK**RRRVTS**RERVARPL), and the other ~30 amino acid residues downstream (RLRSQT). Both sites contain the classical AKT phosphorylation motif RXRXXS/ T with S/T being the amino acid residue targeted for modification (Figure 1A). In order to facilitate phosphorylation site mapping studies, MT396(-P)WT, a truncated DNMT1:EGFP construct beginning at sequence AKSDES (marked with arrow at position ~186), and lacking the PCNA binding region, was created to remove multiple sites of potential phosphorylation. Finally, in order to study the intracellular trafficking by FRAP, we created DNMT1:DsRED in order to alleviate problems with photo-toxicity with laser light wavelengths used during FRAP with EGFP studies. These fluorescently labeled constructs allowed real-time visualization of movements between cellular compartments and permitted the co-immunoprecipitation (using anti-EGFP MAb) of any binding partners. Both EGFP and DsRed constructs behaved in a manner identical to the actual DNMT1 enzyme with respect to its ability to localize to the replication foci, and to translocate to the nucleus as seen in time-lapse confocal imaging experiments (data not shown). However, the MT396(-P)WT construct was not detectable in replication foci due to its lack of a PCNA binding motif (data not shown).

IL-6 stimulated labeling of DNMT1:EGFP expressing 293HEK cells with ^{32}P reveals multiple phosphorylation sites. As previously noted, endogenous DNMT1 is a phosphoprotein, but the only *in vivo* evidence was derived from a twelve hour labeling experiment (27). Numerous attempts to perform mass spectroscopy analysis of endogenous DNMT1 protein derived from transiently stimulated cells proved fruitless (data not shown). In order to study the transient patterns of phosphorylation induced by IL-6, we instead utilized our over-expressed DNMT1 fusion constructs. This strategy allowed us to analyze different substitution mutants, and correlate the effects of each mutation during co-precipitation and FRAP experiments.

HEK293 cells stably expressing the DNMT1:EGFP fusion protein or EGFP protein alone were labeled with ^{32}P-orthophosphate, pulsed with IL-6 for 30 minutes, and lysed with immunoprecipitation buffer. Figure 2A, Lane 1 shows the EGFP control vector immunoprecipitation; no ^{32}P-orthophosphate labeling of the EGFP protein was detected. By contrast, Lane 2 shows a strongly labeled protein band precipitated from cells stably expressing the DNMT1:EGFP construct (Figure 2A).

We then used isoelectric focusing (IEF) SDS-PAGE 2-dimensional gels to better separate phosphorylated DNMT1 proteins in our immunoprecipitations for further analysis. The identical regions of unstimulated (Figure 2B-2) and IL-6 stimulated (Figure 2B-1) gels, revealed that the DNMT1:EGFP fusion protein is phosphorylated and present in multiple species following IL-6 stimulation as determined by the incorporation of phosphoprotein specific Diamond Stain®, and by the shift of the protein spots toward the electronegative pole of the gel. This type of pattern indicates IL-6 was responsible for the generation of multiple phosphorylated species (35). The unstimulated cells did not show any significant incorporation of the Diamond Stain® in the immunoprecipitated DNMT1:EGFP protein.

Next, the DNMT1:EGFP fusion protein was excised from another 2D gel and subjected to proteolytic digestion. Mass spectroscopic (MS) analysis revealed that at least one of the

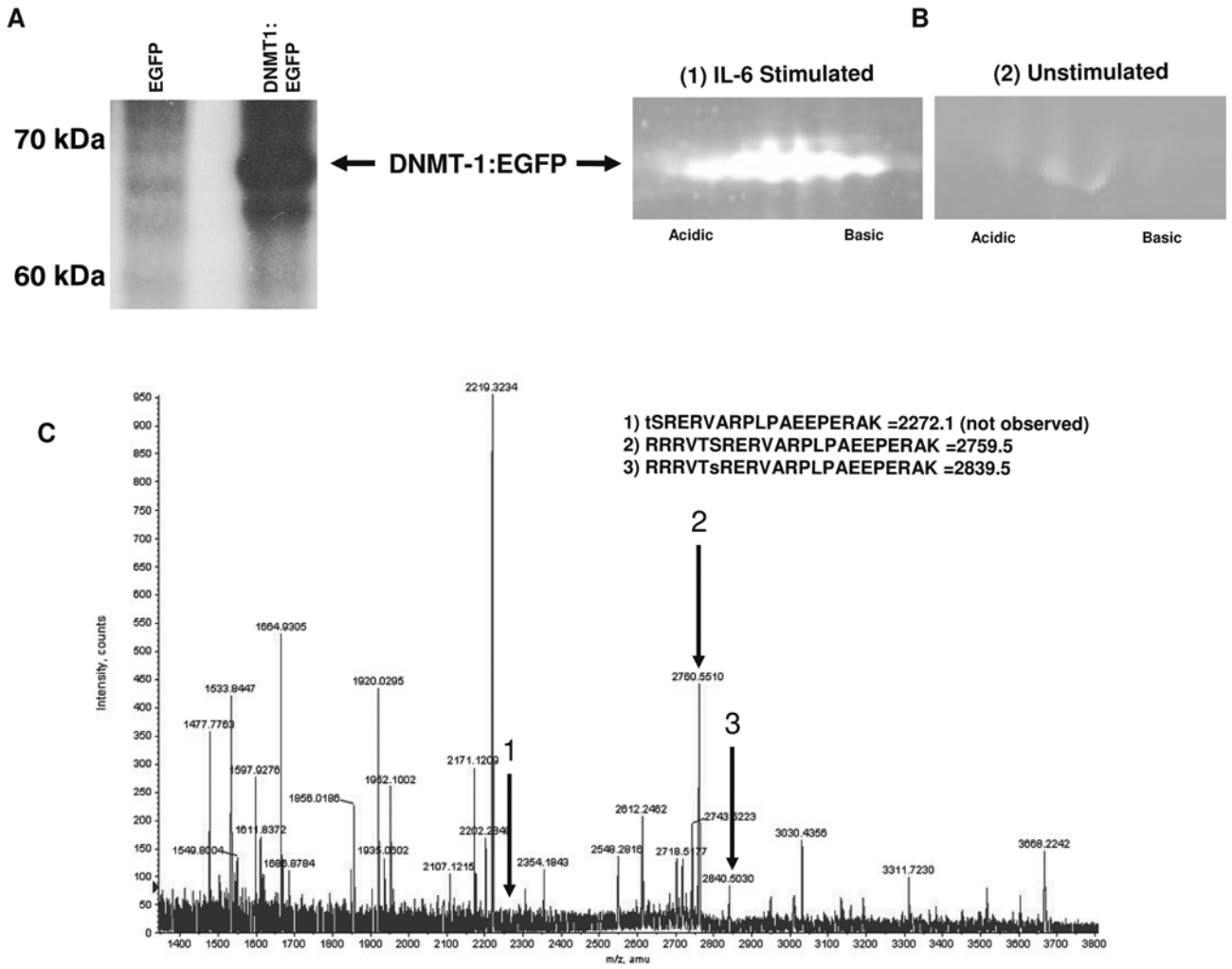

Figure 2. *IL-6 stimulated labeling of DNMT1:EGFP expressing 293HEK cells with ^{32}P reveals multiple phosphorylation sites. Panel A, labeling of 293HEK cells with ^{32}P, followed by immunoprecipitation (IP) of EGFP and DNMT1:EGFP fusion protein. Lane 1 EGFP vector only; Lane 2, ^{32}P-labeled DNMT1:EGFP fusion protein. Panel B, Relevant portion of an IEF-SDS-PAGE 2-dimensional gel showing the immunoprecipitated DNMT1:EGFP fusion protein from IL-6 stimulated (1) and unstimulated (2) cells. Diamond Stain® is specific for phosphorylated proteins, and demonstrates multiple phosphorylated species. Panel C, Mass spectroscopy analysis of DNMT1:EGFP fusion protein spots cut from Panel B gel, followed by proteolytic digestion, revealed at least one of the predicted AKT sites (RRRVTs) was phosphorylated. Numbered arrows designate Peptide 3, which contains a phosphorylated residue (RRRVTsRERVARPLPAEEPERAK=2839.5 D), and its unphosphorylated counterpart, Peptide 2. Peptide 1, containing a phosphorylated threonine residue (tSRERVARPLPAEEPERAK =2272.1 D) was not observed, thereby pinpointing the site of modification as the serine residue.*

predicted AKT sites (RRRVTs) was phosphorylated (Figure 2C). The peptide (Figure 2C, Arrow 3) containing the putative phosphorylated residue (RRRVT*s*RERVARP LPAEEP ERAK) is shown, having an atomic mass unit value (AMU) of 2839.5. Also detected was the corresponding unphosphorylated peptide (Figure 2C, Arrow 2) (RRRVT SRERVARPLPAEEPERAK), with an AMU of 2759.5, approximately 80 AMU less than its phosphorylated counterpart. This peptide contains two potential amino acid target sites for post-translational modification (*i.e.*, T or S). The peptide containing a phosphorylated threonine residue (Figure 2C, Arrow 1) (*t*SRERVARPLPAEEPERAK =2272.1) was not observed; strongly suggesting the site of post-translational modification was most likely the serine residue. A peptide containing the other predicted AKT site (RLRSQ*T*) was not observed in the MS spectra; however, this result is not unusual, since proteolytic sites in target proteins do not always fall in positions conveniently detectable by MS.

In vivo phospholabeling of full-length and truncated DNMT1:EGFP fusion proteins. To further determine the exact positions of any phosphorylated amino acids present in

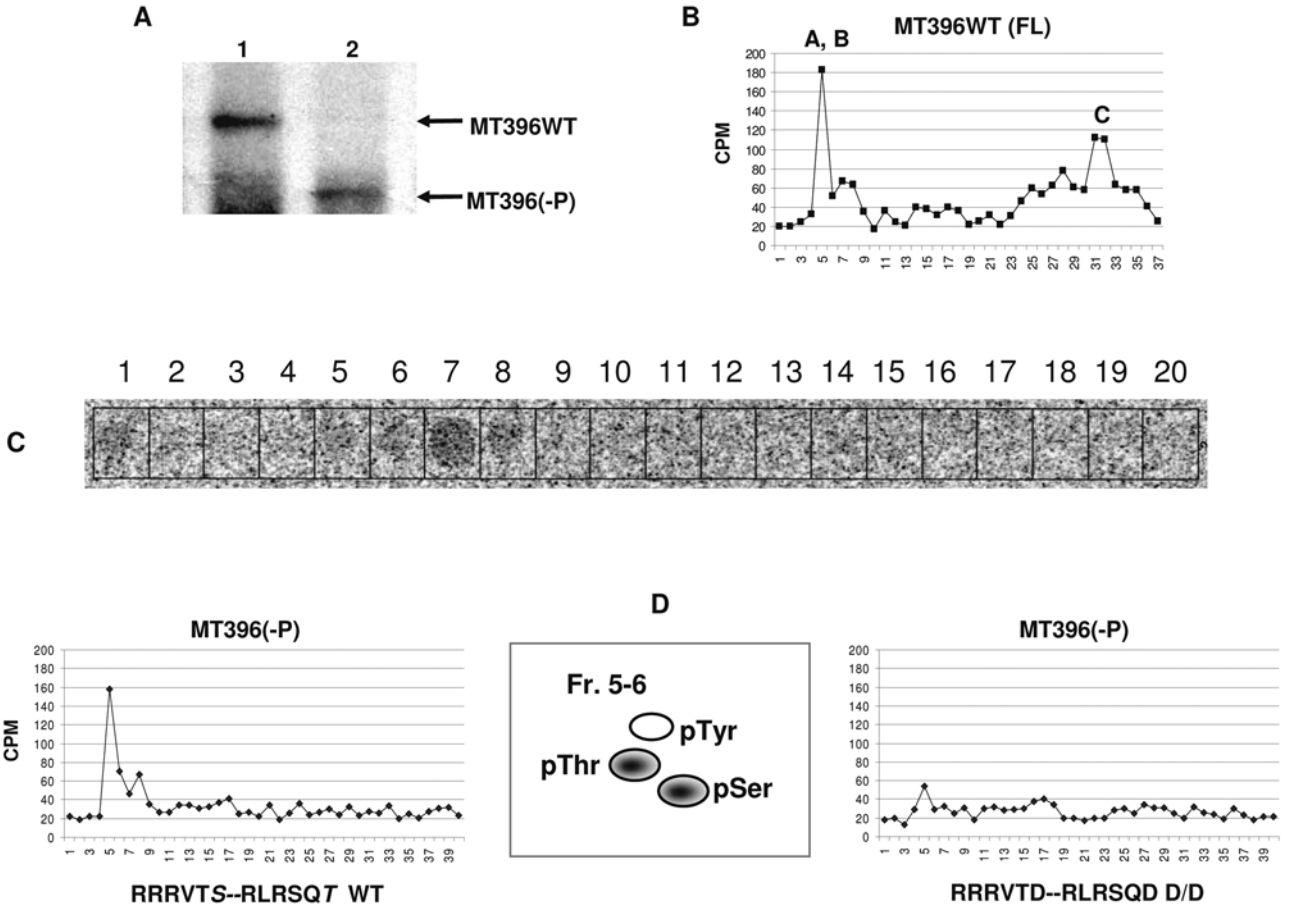

Figure 3. *A) In vivo phospholabeling of full-length and truncated DNMT1:EGFP fusion proteins. In vivo phospholabeling of DNMT1:EGFP full-length (WT) and truncated (-P) fusion proteins, protein bands are indicated by arrows. Bands were extracted from gel, digested with Glu-C protease, and separated by HPLC with beta-counter monitoring of eluted fractions. Panel B, As predicted by peptide mapping of the DNMT1 amino acid sequence, the proteolytic digestion of the recovered DNMT1:EGFP fusion proteins with Glu-C protease released two nine-amino-acid peptides with nearly identical composition, A and B, both containing putative AKT sites, with a ^{32}P-labeled amino acid at position seven as shown by Edman degradation analysis in Panel C. D) A ^{32}P-labeled Peptide C (fractions ~30-33 in B) disappears when the PCNA binding site is deleted (left chromatogram), while A and B peptides remain intact. Phospho-amino acid analysis shows both serine (RRRVTs) and threonine (RLRSQt) are ^{32}P-labeled (center). Mutation of these two putative AKT target site amino acids abrogates labeling of the A and B peptides in right chromatogram.*

the region of the NLS, we ^{32}P-labeled DNMT1:EGFP full-length and truncated fusion proteins and immuno-precipitated them from IL-6 stimulated cells (Figure 3A, Lanes 1 and 2, respectively). Proteolytic digestion of the excised ^{32}P-labeled proteins with Glu-C protease, followed by HPLC analysis of cleaved peptides, released (as predicted by peptide cleavage mapping and shown in Figure 1A) two nearly identical nine amino acid long peptides (A & B), and a larger peptide (C) containing a region previously reported to bind the PCNA protein (Figure 3B). Peptide C (fractions ~30-35 in Figure 3B), disappears when the PCNA binding site is deleted (Figure 3D, left and right panels). Peptides A and B, both containing putative AKT sites, eluted as a single, major peak, which was subjected to sequential Edman degradation, with each eluted residue blotted onto a filter for detection by beta-counting; a ^{32}P-labeled amino acid residue at position seven was detected (Figure 3C). A portion of this A/B peak was retained and the peptides were hydrolyzed, followed by 2D phosphoamino-acid analysis; revealing that both serine and threonine residues were labeled (Figure 3D, center panel). These two results (Figure 3B and C) prove that the predicted AKT kinase target residues (a serine and a threonine each residing at position seven in the Glu-C peptides) were present in a phosphorylated state.

Figure 3D also shows that mutation of both putative AKT target amino acid residues in the PCNA truncated mutant, MT396(-P)WT, (designated as the D/D mutant, right panel)

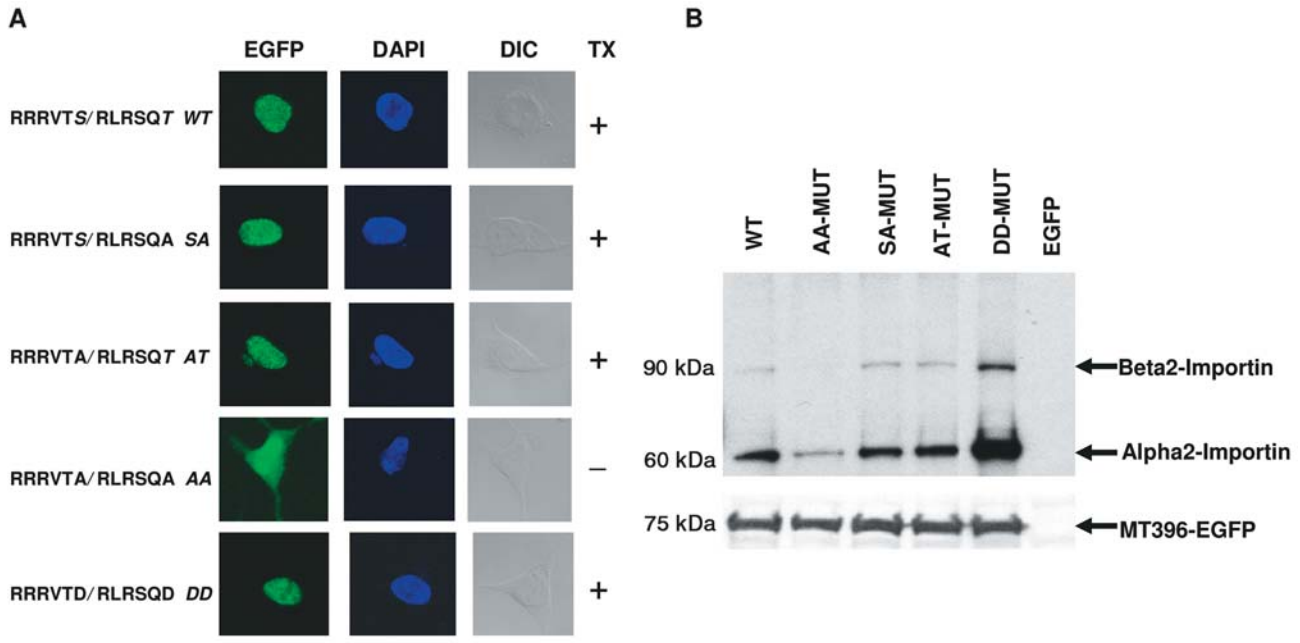

Figure 4. *A) AKT sites near the nuclear localization signal (NLS) affect translocation and binding affinity for importins. The nuclear translocation (TX) of the wild-type and several mutant DNMT1:EGFP fusion proteins is shown along with DAPI and phase-contrast photos for comparison. Translocation of the double AKT site mutant, AA, is greatly diminished. Interestingly, the analogous double AKT mutant "DD," containing two aspartic acid residues at the putative AKT target residues does localize to the nucleus, indicating that these two acidic residues are probably mimicing phosphorylation sites. B) Co-precipitation experiments with the same proteins, suggests phosphorylation of the AKT sites around NLS affects the binding to Importins. Western blotting of IP using several different DNMT1:EGFP fusion proteins as bait, demonstrate the binding of alpha- and beta-importins were affected by mutation of AKT target sites. Both alpha2- and beta2-importins co-precipitate with the wild-type and other mutant DNMT1:EGFP fusion proteins, with the exception of the AA mutant. Again, the DD mutant binds both the alpha- and beta-importins very strongly. A control Western blot using anti-EGFP MAb shows the equivalent loading of each sample, with the 6th lane representing the EGFP expression plasmid alone; hence no band is observed in the control blot at ~75 kDa.*

abrogated the labeling of both peptides by ^{32}P in comparison to the wild-type construct (left panel).

AKT sites near the nuclear localization signal (NLS) affect translocation and binding affinity for importins. We next sought to correlate the phosphorylation status of the two AKT target sites with ability of the protein to translocate from the cytoplasm to the nucleus. Single and double point mutations of the AKT kinase target residues within the DNMT1:EGFP fusion protein NLS were created, as described (*i.e.*, either an alanine or aspartic acid residue was substituted for the phospho-accepting AKT target residues). Plasmids expressing the wild-type, and several AKT site mutated DNMT1:EGFP fusion proteins were transfected into HEK293 cells. Confocal microscope images showing the EGFP, DAPI (nuclear) and differential interference contrast (DIC) images for each protein appear in Figure 4A. All proteins translocated to the nucleus except the double mutant, "AA," in which both phospho-accepting serine and threonine residues were mutated to alanines (Figure 4A, 4th set of panels). However, the double mutant "DD," containing two aspartic acid residues at the putative AKT target sites localized to the nucleus (Figure 4A, bottom panels,). The negatively charged phospho-mimicing amino acid residues apparently provide a viable substitute for phosphorylation, further confirming the importance of phosphorylation in the nuclear translocation of DNMT1. In experiments where only one AKT kinase target residue was mutated and the other left intact (Figure 4A, 2nd and 3rd panels), the DNMT1:EGFP fusion protein was still able to translocate to the nucleus.

Using the same panel of mutated DNMT1:EGFP fusion constructs (Figure 4A) as bait-proteins, we next studied the effect the AKT site mutations had on the ability of each protein to co-precipitate the alpha- and beta-importins, known transporters of "cargo" proteins through the nuclear pores. Figure 4B shows mutation of both AKT target sites (AA mutant) greatly reduces binding of both alpha- and beta-importins. Conversely, the mutation of both AKT target sites to aspartic acids (DD mutant) yielded a mutant protein that appears to bind both alpha- and beta-importins more efficiently than did the wild-type protein. We suspect this increase in binding efficiency is due to the fact that the DD bait protein appears fully phosphorylated and thus binds a greater percentage of the available alpha- and beta-

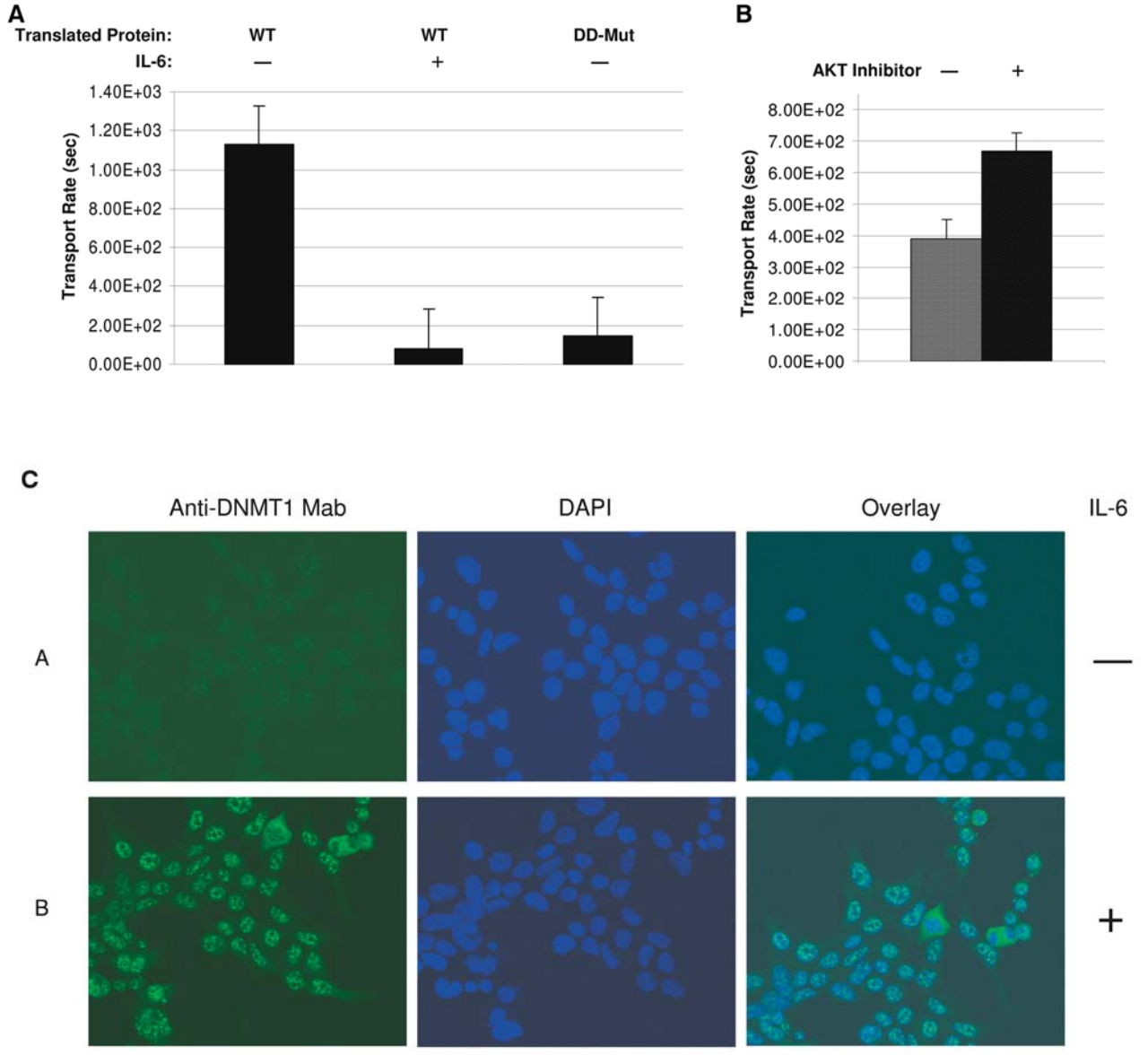

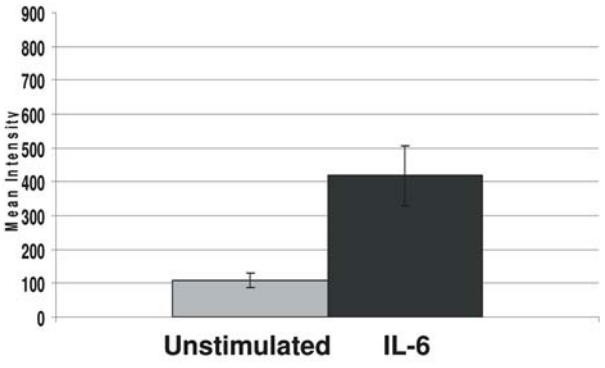

Figure 5. *A) Translocation rate of DNMT1 is mediated by IL-6. Fluorescent recovery after photobleaching (FRAP) was performed on cells expressing wild-type or DD mutant DNMT1:EGFP fusion proteins to determine real-time rates of nuclear translocation following IL-6 treatment. The rates of cytoplasmic to nuclear transport increased with IL-6 stimulation of cells transfected with the wild-type DNMT1:EGFP fusion protein (Bar 1, unstimulated, Bar 2, IL-6 treated). However, the DD mutant (Bar 3) reflects the same transport characteristics in unstimulated cells as when IL-6 stimulation is present. B) Use of a specific AKT inhibitor slows the transport rate of the wild-type DNMT1:EGFP fusion protein, indicating the involvement of the kinase in the nuclear translocation of the enzyme. C) HEK293 cells were rested overnight without serum, then stimulated for four hours with 100 ng/mL IL-6; fixed and incubated with anti-DNMT1 MAb as described in the Materials and Methods section. Part A shows immunohistochemical staining of DNMT1 in unstimulated cells; Part B shows an increase in DNMT1 nuclear localization following IL-6 treatment, and this increase in staining intensity is quantified in the graph below.*

importins. Collectively, these observations support the idea that only one NLS site is required for nuclear translocation; loss of a single AKT target site (SA and AT mutants) does not appear to hinder nuclear transport or importin binding.

Translocation rate of DNMT1 is mediated by IL-6 induced phosphorylation. Finally, we sought to determine the temporal aspects of IL-6 stimulation on DNMT1 nuclear translocation, using confocal microscopy, and fluorescent recovery after photobleaching (FRAP). A DNMT1:dsRED construct was chosen to reduce photo-toxicity for our study of translocation rates in live cells. As shown in Figure 5A, the rates of cytoplasmic to nuclear transport dramatically increased with IL-6 stimulation of cells (100 ng/mL IL-6 for 30 minutes) ($8.07x10^1$ seconds) (Lane 2) transfected with the wild-type DNMT1:dsRED fusion protein in contrast to no stimulation ($1.13x10^3$ seconds) (Lane 1). This short time frame precludes the possibility of *de novo* synthesis of proteins, and demonstrates a dramatic IL-6 mediated increase in nuclear translocation of the DNMT1:dsRED fusion proteins. Even more revealing was the effect on nuclear translocation exerted by the two acidic mutations present in the DD mutant DNMT1:dsRED fusion protein (Figure 5A, Lane 3), which closely imitate the IL-6 induced accelerated transport only in unstimulated cells ($1.44x10^2$ seconds for the unstimulated DD mutant compared to $8.07x10^1$ seconds for the IL-6 stimulated wild-type DNMT1:dsRED). Next, we used the AKT kinase inhibitor Triciribine at a concentration of 1 μM to ascertain its effect on nuclear translocation of DNMT1:dsRED following IL-6 stimulation as in 5A. The cells in this experiment were allowed to incubate 4x longer in IL-6 prior to the addition of the drug in order to protect them from apoptosis. Figure 5B shows an approximately 40% reduction in the rate of nuclear translocation in the Triciribine treated cells (Lane 2) as compared to the untreated wild-type DNMT1:dsRED construct (Lane 1).

To demonstrate the effects of IL-6 on the endogenous DNMT1 protein HEK293 cells were serum deprived overnight, followed by four hours of IL-6 stimulation (100 ng/mL), then immediately fixed and stained with anti-DNMT1 monoclonal antibody. The basal level of DNMT1 present in unstimulated, negative control cells is shown in Figure 5C, Panel A, while Panel B shows the IL-6 stimulated cells. An increase of approximately 3.8-fold in DNMT1 nuclear localization pixel intensity is noted following IL-6 treatment, and is depicted in the graph beneath the photographs.

Discussion

The signaling pathways that mediate acute inflammatory responses allow the immune system to respond to pathogenic organisms, which otherwise would cause serious harm or even death to the host. Unfortunately, the same system of cytokine and chemokine factors responsible for protecting cells during the transient inflammatory response, are often responsible for producing unintended consequences such as blocking apoptosis in pre-cancerous and tumor cells (36), which is associated with chronic inflammatory conditions. The connection between inflammation and cancer has been known for decades, yet the actual mechanisms responsible for the step-by-step progression to neoplasia are poorly characterized (37). The ability of cytokines such as IL-6 to produce important changes in cellular expression patterns is also becoming clearer, and this major inflammatory cytokine has been implicated in the progression and survival of many types of tumors and cancers (38).

The epigenetic programming of cells also represents an important control mechanism, the dysregulation of which appears to contribute to increasingly detrimental events in pre-cancerous and malignant cells (39), ultimately causing the loss of expression of tumor suppressor genes, regulators of reduction-oxidation reactions, DNA repairs genes, and important mediators of apoptosis (40, 41). The bulk of the evidence that epigenetic dysregulation contributes to cancer is represented primarily through experimental work demonstrating the presence of abnormal patterns of methylation in the promoters of important tumor suppressor genes (5, 42).

In this study, we show for the first time that one of the contributing factors to dysregulation of the epigenetic program may be driven by IL-6 activation of the PI-3/AKT kinase pathway, resulting in discreet changes in the normal cellular compartmentalization and distribution of the DNMT1 enzyme. Knowing that the AKT kinase, a downstream target of IL-6 mediated stimulation of the PI-3 kinase, inactivated $p21^{WAF1/CIP1}$ (a protein in competition with DNMT1 to bind PCNA), we hypothesized that perhaps a post-translational modification of DNMT1 might also occur in response to IL-6 stimulation of the AKT pathway. Furthermore, there are many reports showing that active AKT favors the growth of tumors, and so we examined the possibility that IL-6 mediated increases in AKT activity might be involved in the phenomenon of epigenetic dysregulation.

Regulation of nuclear transport is often mediated by various kinases, which in turn can be modulated by many competing extracellular signals. Since the proper cellular localization of proteins appears, in some cases, to depend upon the phosphorylation status of the nuclear import (or export) signals, this phenomenon represents a direct link between abnormal external signaling and the mislocalization of an important protein of oncogenic potential (24, 25). We have already demonstrated alterations in both expression levels and activity of DNMT1 following exposure to IL-6. It now appears that some of these changes in activity might be due to phosphorylation of the enzyme following exposure to IL-6, and the subsequent activation of downstream signaling

pathways. Indeed, the mutagenic alterations of the two NLS sites of DNMT1 clearly demonstrated that removing the AKT target sites greatly reduced the rate of DNMT1:EGFP fusion protein cytoplasmic-to-nuclear transport. However, when the same sites were converted to acidic residues, resembling the phosphorylated state of the AKT target residue, the DNMT1 fusion protein behaved as if it were phosphorylated, and bound much higher levels of the importin proteins. We surmise this increased affinity is due to the structural changes induced by either phosphorylation or mutation to acidic residues, in NLS of the DNMT1 enzyme making it a more attractive and stable binding partner for the importins.

Based on these data, we predict that long-term exposure to IL-6, even at low-levels, could lead to the induction of aberrant epigenetic effects by DNMT1, mediated by the cytokine's ability to activate the AKT pathway, thus inducing improper cellular localization of this enzyme. These effects would probably not be readily noticeable early in chronic viral infections (*e.g.*, HBV, HPV, are both implicated in tumor development). However, following extended and ineffectual immune responses producing constant low-grade inflammatory states, the presence of inflammatory cytokines could be capable of triggering the actions we describe, leading to more permanent epigenetic events. We note with great interest that many pathological conditions including colitis (43), pancreatitis (44), and gastritis (45) all presage the development of tumors in each respective tissue type. The alterations in the epigenetic programming of cells, both in the process of moving towards neoplasia, and those already existing as tumors, exhibit a continuum of methylation problems, starting with minor aberrations and ending with major alterations (7, 46).

Our observations raise interesting questions regarding similar changes in nuclear translocation rates induced by other growth or survival factors known to be involved in driving cells into neoplastic states. Whether chronic exposure to IL-6 is capable of inducing changes in epigenetic programming by mechanisms of mislocalization of nuclear proteins requires further investigation. The results we have presented potentially link abnormal DNMT1 nuclear localization with IL-6 induced AKT activation, and strengthens the current speculation on whether inflammation (or its mediators) causes or exacerbates neoplastic growth and cancer.

References

1 Woodcock DM, Crowther PJ and Diver WP: The majority of methylated deoxycytidines in human DNA are not in the CpG dinucleotide. Biochem Biophys Res Commun *145*: 888-894, 1987.

2 Michalowsky LA and Jones PA: DNA methylation and differentiation. Environ.Health Perspect *80*: 189-197, 1989.

3 Kimura H and Shiota K: Methyl-CpG-binding protein, MeCP2, is a target molecule for maintenance DNA methyltransferase, Dnmt1. J Biol Chem *278*: 4806-4812, 2003.

4 Robertson KD: DNA methylation, methyltransferases and cancer. Oncogene *20*: 3139-3155, 2001.

5 Karpf AR and Jones DA: Reactivating the expression of methylation silenced genes in human cancer. Oncogene *21*: 5496-5503, 2002.

6 Majumder S, Ghoshal K, Datta J, Bai S, Dong X, Quan N, Plass C and Jacob ST: Role of *de novo* DNA methyltransferases and methyl CpG-binding proteins in gene silencing in a rat hepatoma. J Biol Chem *277*: 16048-16058, 2002.

7 De Marzo AM, Marchi VL, Yang ES, Veeraswamy R, Lin X and Nelson WG: Abnormal regulation of DNA methyltransferase expression during colorectal carcinogenesis. Cancer Res *59*: 3855-3860, 1999.

8 Jee SH, Chu CY, Chiu HC, Huang YL, Tsai WL, Liao YH and Kuo ML: Interleukin-6 induced basic fibroblast growth factor-dependent angiogenesis in basal cell carcinoma cell line *via* JAK/STAT3 and PI3-kinase/Akt pathways. J Invest Dermatol *123*: 1169-1175, 2004.

9 Yang L, Wang L, Lin HK, Kan PY, Xie S, Tsai MY, Wang PH, Chen YT and Chang C: Interleukin-6 differentially regulates androgen receptor transactivation *via* PI3K-Akt, STAT3, and MAPK, three distinct signal pathways in prostate cancer cells. Biochem Biophys Res Commun *305*: 462-469, 2003.

10 Hodge DR, Li D, Qi SM and Farrar W: L. IL-6 induces expression of the Fli-1 proto-oncogene *via* STAT3. Biochem Biophys Res Commun *292*: 287-291, 2002.

11 Hodge DR, Xiao W, Clausen PA, Heidecker G, Szyf M and Farrar WL: Interleukin-6 regulation of the human DNA methyltransferase (HDNMT) gene in human erythroleukemia cells. J Biol Chem *276*: 39508-39511, 2001.

12 Hodge DR, Peng B, Cherry JC, Hurt EM, Fox SD, Kelley JA, Munroe DJ and Farrar WL: Interleukin 6 supports the maintenance of p53 tumor suppressor gene promoter methylation. Cancer Res *65*: 4673-4682, 2005.

13 Wehbe H, Henson R, Meng F, Mize-Berge J and Patel T: Interleukin-6 contributes to growth in cholangiocarcinoma cells by aberrant promoter methylation and gene expression. Cancer Res *66*: 10517-10524, 2006.

14 Amorino GP and Parsons SJ: Neuroendocrine cells in prostate cancer. Crit Rev Eukaryot Gene Expr *14*: 287-300, 2004.

15 Hideshima T, Nakamura N, Chauhan D and Anderson KC: Biologic sequelae of interleukin-6 induced PI3-K/Akt signaling in multiple myeloma. Oncogene *20*: 5991-6000, 2001.

16 Zhou BP, Liao Y, Xia W, Spohn B, Lee MH and Hung MC: Cytoplasmic localization of $p21^{Cip1/WAF1}$ by Akt-induced phosphorylation in HER-2/neu-overexpressing cells. Nat Cell Biol *3*: 245-252, 2001.

17 Zhou BP, Liao Y, Xia W, Spohn B, Lee MH and Hung MC: Cytoplasmic localization of $p21^{Cip1/WAF1}$ by Akt-induced phosphorylation in HER-2/neu-overexpressing cells. Nat Cell Biol *3*: 245-252, 2001.

18 Liang J, Zubovitz J, Petrocelli T, Kotchetkov R, Connor MK, Han K, Lee JH, Ciarallo S, Catzavelos C, Beniston R, Franssen E and Slingerland JM: PKB/Akt phosphorylates p27, impairs nuclear import of p27 and opposes p27-mediated G1 arrest. Nat Med *8*: 1153-1160, 2002.

19 Zhou BP, Liao Y, Xia W, Zou Y, Spohn B and Hung MC: HER-2/neu induces p53 ubiquitination *via* Akt-mediated MDM2 phosphorylation. Nat Cell Biol *3*: 973-982, 2001.
20 Iida T, Suetake I, Tajima S, Morioka H, Ohta S, Obuse C and Tsurimoto T: PCNA clamp facilitates action of DNA cytosine methyltransferase 1 on hemimethylated DNA. Genes Cells *7*: 997-1007, 2002.
21 Cardoso MC and Leonhardt H: DNA methyltransferase is actively retained in the cytoplasm during early development. J Cell Biol *147*: 25-32, 1999.
22 Faul C, Huttelmaier S, Oh J, Hachet V, Singer RH and Mundel P: Promotion of importin alpha-mediated nuclear import by the phosphorylation-dependent binding of cargo protein to 14-3-3. J Cell Biol *169*: 415-424, 2005.
23 Jans DA, Xiao CY and Lam MH: Nuclear targeting signal recognition: a key control point in nuclear transport? Bioessays *22*: 532-544, 2000.
24 Kau TR, Way JC and Silver PA: Nuclear transport and cancer: from mechanism to intervention. Nat Rev Cancer *4*: 106-117, 2004.
25 Kau TR and Silver PA: Nuclear transport as a target for cell growth. Drug Discov Today *8*: 78-85, 2003.
26 DePaoli-Roach A, Roach PJ, Zucker KE and Smith SS: Selective phosphorylation of human DNA methyltransferase by protein kinase C. FEBS Lett *197*: 149-153, 1986.
27 Glickman JF, Pavlovich JG and Reich NO: Peptide mapping of the murine DNA methyltransferase reveals a major phosphorylation site and the start of translation. J Biol Chem *272*: 17851-17857, 1997.
28 Elias B, Laine A and Ronai Z: Phosphorylation of MdmX by CDK2/Cdc2(p34) is required for nuclear export of Mdm2. Oncogene *24*: 2574-2579, 2005.
29 Houtsmuller AB: Fluorescence recovery after photobleaching: application to nuclear proteins. Adv Biochem Eng Biotechnol *95*: 177-199, 2005.
30 Carrero G, McDonald D, Crawford E, de Vries G and Hendzel MJ: Using FRAP and mathematical modeling to determine the *in vivo* kinetics of nuclear proteins. Methods *29*: 14-28, 2003.
31 Yang L, Dan HC, Sun M, Liu Q, Sun XM, Feldman RI, Hamilton AD, Polokoff M, Nicosia SV, Herlyn M, Sebti SM and Cheng J: Q. Akt/protein kinase B signaling inhibitor-2, a selective small molecule inhibitor of Akt signaling with antitumor activity in cancer cells overexpressing Akt. Cancer Res *64*: 4394-4399, 2004.
32 Shevchenko A, Jensen ON, Podtelejnikov AV, Sagliocco F, Wilm M, Vorm O, Mortensen P, Shevchenko A, Boucherie, H and Mann M: Linking genome and proteome by mass spectrometry: large-scale identification of yeast proteins from two dimensional gels. Proc Natl Acad Sci USA *93*: 14440-14445, 1996.
33 Stephens, RM, Sithanandam G, Copeland TD, Kaplan DR, Rapp UR and Morrison DK: 95-kilodalton B-Raf serine/threonine kinase: identification of the protein and its major autophosphorylation site. Mol Cell Biol *12*: 3733-3742, 1992.
34 Morrison DK, Heidecker G, Rapp UR and Copeland TD: Identification of the major phosphorylation sites of the Raf-1 kinase. J Biol Chem *268*: 17309-17316, 1993.
35 Tang HY and Speicher DW: *In vivo* phosphorylation of human erythrocyte spectrin occurs in a sequential manner. Biochemistry *43*: 4251-4262, 2004.
36 Lichtenstein A, Tu Y, Fady C, Vescio R and Berenson J: Interleukin-6 inhibits apoptosis of malignant plasma cells. Cell Immunol *162*: 248-255, 1995.
37 Potter M, Pumphrey JG and Walters JL: Growth of primary plasmacytomas in the mineral oil-conditioned peritoneal environment. J Natl Cancer Inst *49*: 305-308, 1972.
38 Martinez-Maza O and Berek JS: Interleukin 6 and cancer treatment. In Vivo *5*: 583-588, 1991.
39 Nephew KP and Huang TH: Epigenetic gene silencing in cancer initiation and progression. Cancer Lett *190*: 125-133, 2003.
40 Plass C and Soloway PD: DNA methylation, imprinting and cancer. Eur J Hum Genet *10*: 6-16, 2002.
41 Pompeia C, Hodge DR, Plass C, Wu YZ, Marquez VE, Kelley JA and Farrar WL: Microarray analysis of epigenetic silencing of gene expression in the KAS-6/1 multiple myeloma cell line. Cancer Res *64*: 3465-3473, 2004.
42 Robertson KD: DNA methylation, methyltransferases, and cancer. Oncogene *20*: 3139-3155, 2001.
43 Rhodes JM and Campbell BJ: Inflammation and colorectal cancer: IBD-associated and sporadic cancer compared. Trends Mol Med *8*: 10-16, 2002.
44 Whitcomb DC: Inflammation and cancer V. Chronic pancreatitis and pancreatic cancer. Am J Physiol Gastrointest Liver Physiol *287*: G315-G319, 2004.
45 Genta RM: The gastritis connection: prevention and early detection of gastric neoplasms. J Clin Gastroenterol *36*: 44-49, 2003.
46 Issa JP: Epigenetic variation and human disease. J Nutr *132*: 2388S-2392S, 2002.

Received October 23, 2007
Accepted November 1, 2007